Fox, C.P., et al., 2022, Two-pronged kill mechanism at the end-Triassic mass extinction: Geology, https://doi.org/10.1130/G49560.1



# Stratigraphy of the SW UK

The lithological similarity between the St. Audrie's Bay and Lilstock sections allows correlation independent of changes in the organic carbon isotope record (Fig. DR1). Lithological details for the Westbury Formation and Lilstock Formation of the Penarth Group and the Blue Lias Formation of the Lias Group are provided in Fox et al., (2020). Because of the difference in thickness between the sections, the depth profile of St. Audrie's Bay is expanded such that lithological transitions between the two sections correlate and appropriate comparisons can be made, hence a 'St. Audrie's Bay original depth' is given in figures.

# Methods

## Sample Preparation

Samples were collected from the St. Audrie's Bay (51.182833°, -32.286000°) and Lilstock (51.200757°, -3.176389°) outcrops in the southwest of the UK. Weathered surface edges were removed and samples were pre-cleaned with 9:1 DCM:MeOH (Dichloromethane:Methanol) 3 times (15 min) before being crushed to a fine powder using a Rocklabs SRM C+PB rock grinder. All glassware was annealed at 500 °C overnight and all apparatuses were thoroughly rinsed with 9:1 dichloromethane:methanol (DCM:MeOH) solution.

## Bulk organic carbon isotopes and total organic carbon

Sedimentary carbonates were removed from powdered rock samples (<0.5 g) via 2M HCl acid digestion (12 hr). Samples were checked to ensure all inorganic carbon had been removed by adding additional 2M HCl. After digestion, samples were brought to a neutral pH using Milli-Q water, and freeze-dried (minimum 12 hr) to remove excess water. Total organic carbon (TOC, %) contents and carbon isotope measurements on the composition of bulk organic matter ($\delta^{13}C_{org}$) were conducted at the West Australian Biogeochemistry Centre, University of Western Australia using a CNHS elemental analyzer and Delta V Plus MS connected to a Thermo Flash 1112 via a Conflo IV, respectively. Full details for elemental analysis can be found in Skrzypek and Debajyoti, 2006 and Skrzypek, 2013.

**Extraction and separation of biomarkers**

Powdered rock samples (between ca 30 – 150 g) were extracted for bitumen compounds using a Milestone Start-E microwave extraction system (21 °C to 80 °C over 10 mins, held at 80 °C for 15 mins) in 9:1 DCM:MeOH (50 mL). Samples were extracted twice, where necessary, to ensure complete extraction of organic material. Activated copper turnings (sonicated for 30 mins in 2M HCl, brought to a neutral pH using Milli-Q water, cleaned using 9:1 DCM:MeOH) were used to remove elemental sulfur. Total bitumen extracts were then fractionated by activated silica gel (heated to 80 °C overnight) chromatography into saturate (*n*-hexane), aromatic (3:1 *n*-hexane:DCM) and polar (9:1 DCM:MeOH) fractions. St. Audrie's Bay saturated fractions were analyzed using an Agilent 6890N gas chromatograph (GC) fitted with a DB-1 (60 m length, 0.25 mm diameter, 0.25 μm film thickness) capillary column (temperature program of 4 °C/min from 50 °C to 325 °C, held at 325 °C for 24 mins), connected to a Micromass Autospec Ultima multiple reaction monitoring mass spectrometer (MRM-MS). Helium was used as a carrier gas (constant flow 1.1 mL/min). St. Audrie's Bay aromatic and Lilstock combined saturate and aromatic fractions were analyzed using an Agilent 7890B GC fitted with a DB-5 (60 m length, 0.25 mm diameter, 0.25 μm film thickness) capillary column (temperature program of 4 °C/min from 40 °C to 325 °C, held at 325 °C for 20.27 mins) connected to an Agilent 7010B triple quadrupole MS. Helium was used as a carrier gas (constant flow 1.1 mL/min). Compounds were identified using the GEOMARK standard and comparing peak retention times and elution patterns, and quantified using internal standards (D4 stigmastane for saturate compounds and D10 phenanthrene for aromatic compounds). Sample preparation was conducted at Curtin University, Australia and biomarker analysis was conducted at the Summons Lab, Massachusetts Institute of Technology.

Compound Specific Isotope Analysis (CSIA) was conducted at Curtin University, Australia using a Thermo Trace GC Ultra fitted with a DB-1MS column (60 m length, 0.25 mm diameter, 0.25 μm film thickness), coupled to a Thermo Delta V Advantage isotope ratio MS via a GC Isolink and Conflo IV. Helium was used as a carrier gas (constant flow 1.1 mL/min). Carbon isotope composition of compounds was achieved using the 44, 45, and 46 masses, which were run in triplicate and integrated manually. Prior to CSIA, samples were run on an Agilent 6890 GC (temperature program of 3 °C/min from 40 °C to 325 °C, held at 325 °C for 30 mins) fitted with a DB-1 capillary column (60 m length, 0.25 mm diameter, 0.25 μm film thickness) interfaced to an Agilent 5973 MS. Helium was used as a carrier gas (constant flow 1.1 mL/min).

**Rock-Eval analysis**

Rock Eval analysis was undertaken at Oxford University using a Vinci Technologies Rock-Eval 6 standard analyzer unit 43, with pyrolysis and oxidation ovens, a flame ionization detector, and 44 infra-red cell. Temperature profiles were 300 to 650 °C and 300 to 850 °C for pyrolysis and oxidation ovens, respectively. Laboratory methods followed those of Behar et al., (2001), and samples were run with the IFP 160000 and in-house (SAB134; organic rich marl) standards.

## Biomarkers

The biomarkers used in this study are presented as either a ratio or a percentage/index. Table DR1 gives the MRM reactions (where applicable) and equations used to generate the biomarker data and the typical precursor for each biomarker compounds. Note that $C_{40}$ carotenoid compounds are compared to triaromatic steroids (TAS). Normalization of aromatic compounds using TAS was undertaken because 1) St. Audrie's Bay saturate fractions were measured by a Waters Autospec in GC-MRM mode whereas aromatic fractions were measured by an Agilent GC-QQQ (due to the former instrument ceasing to function correctly); and 2) total extracted lipids were fractionated into saturated, aromatic, and polar fractions. Thus, normalization of $C_{40}$ carotenoid compounds against another group of aromatic compounds was required to reduce stratigraphic bias, hence $C_{26\text{-}28}$ TAS (compounds originating from algae but have different diagenetic pathways compared to the saturated sterane compounds) were chosen. For further quality control, AGSO and GeoMark II oil standards were measured in the sample sequences on both instruments, and the Agilent GC-QQQ instrument is setup to attain the same chromatographic patterns as the Waters Autospec. Biomarkers indicating stratification, redox, and photic zone euxinia are given in the main text, whereas full biomarker profiles indicating changes to eukaryotes and select bacteria are given in Fig. DR2 an those of redox conditions given in Fig. DR3.

## Rock Eval pyrolysis

Rock-Eval pyrolysis is used to determine the H/C and O/C measurements on bulk organic matter, and typically used to evaluate the petroleum-generative potential, thermal maturity and type of source rocks. Organic matter can be broadly divided into four categories (Types I through IV). Type I kerogen, characterized by a very high hydrogen index (HI) and low oxygen index (OI) values, is generally ascribed to well preserved organic matter from algal origin, although it can also include the liptinitic components of vascular plants from lacustrine settings. Type II is generally comprised of amorphous or structureless organic matter and is the result of bacterial reworking of primary algal material in addition to the preserved bacterial organic matter, or a combination of all types of kerogen that plot as type II in the van Krevelen diagram. Type III kerogen is sourced from either vitrinite (a primary component of coals), high plant material and/or poorly preserved/partially oxidized algal or amorphous organic matter. Type IV generally

implies heavily oxidized and/or poorly preserved organic matter. Kerogen type is dependent on the mix, end members and preservation state of the various organic components and limited to immature to low maturity samples. Our samples are in this range, with maximum temperatures ($T_{max}$) between 418°C and 435°C and production indexes (PI) between 0.00 and 0.14 (Table DR2). Kerogen type of these samples range between type II and type III-IV (Fig. DR4).

## Episodic vs. Persistent PZE

A cross plot of the aryl isoprenoid ratio (AIR) and pristane to phytane ratio (Pr/Ph) determines whether intervals of PZE were persistent or episodic (Fig. DR5). Pristane and phytane are generally formed from the phytyl side chain of chlorophyll *a* under oxic and anoxic conditions, respectively (e.g., Grice *et al.*, 1996), thus low ratios indicate anoxia. The $C_{13-31}$ aryl isoprenoids are formed from carotenoid pigments produced by Chromatiaceae and Chlorobi that utilize $H_2S$ in the photic zone of the water column. The AIR is calculated from the ratio of $C_{13-17}$ to $C_{18-22}$ aryl isoprenoids. Because the concentrations of aryl isoprenoids in euxinic conditions correlate negatively to the AIR, consistent with degradation and diagenesis, the AIR is a good indication of persistent PZE when values are low, ~0.5 (Schwark and Frimmel, 2004; Jaraula et al., 2013). For the SW UK, samples during the calcification crisis plot close towards zero (Fig. DR5) indicating persistent PZE. Aryl isoprenoids can have multiple sources, therefore, the AIR is only calculated when total PZE biomarkers and total $C_{13-22}$ aryl isoprenoids abundances are high. Note that those samples from within the Bristol Channel Basin carbon isotope excursion are not included because of their microbial-mat related origin (see Fox et al., 2020).

## Bivalves

The bivalves recorded by Mander et al., (2008) and Atkinson and Wignall, (2019) in the St. Audrie's Bay section represent different groups that diverge in their mobility (stationary, mobile) and habitat (infaunal and epifaunal). A full list of the bivalves observed at St. Audrie's Bay and their ecology is given in Table DR4. A combination of proxies for PZfE from this study and others are compared to the SW UK bivalve assemblages amongst other fossil taxa (Fig. DR6). Note that the largest expansion in calcifying fossil assemblages occurs after the paper shales of the Blue Lias Formation and in close proximity to the return of ammonites.

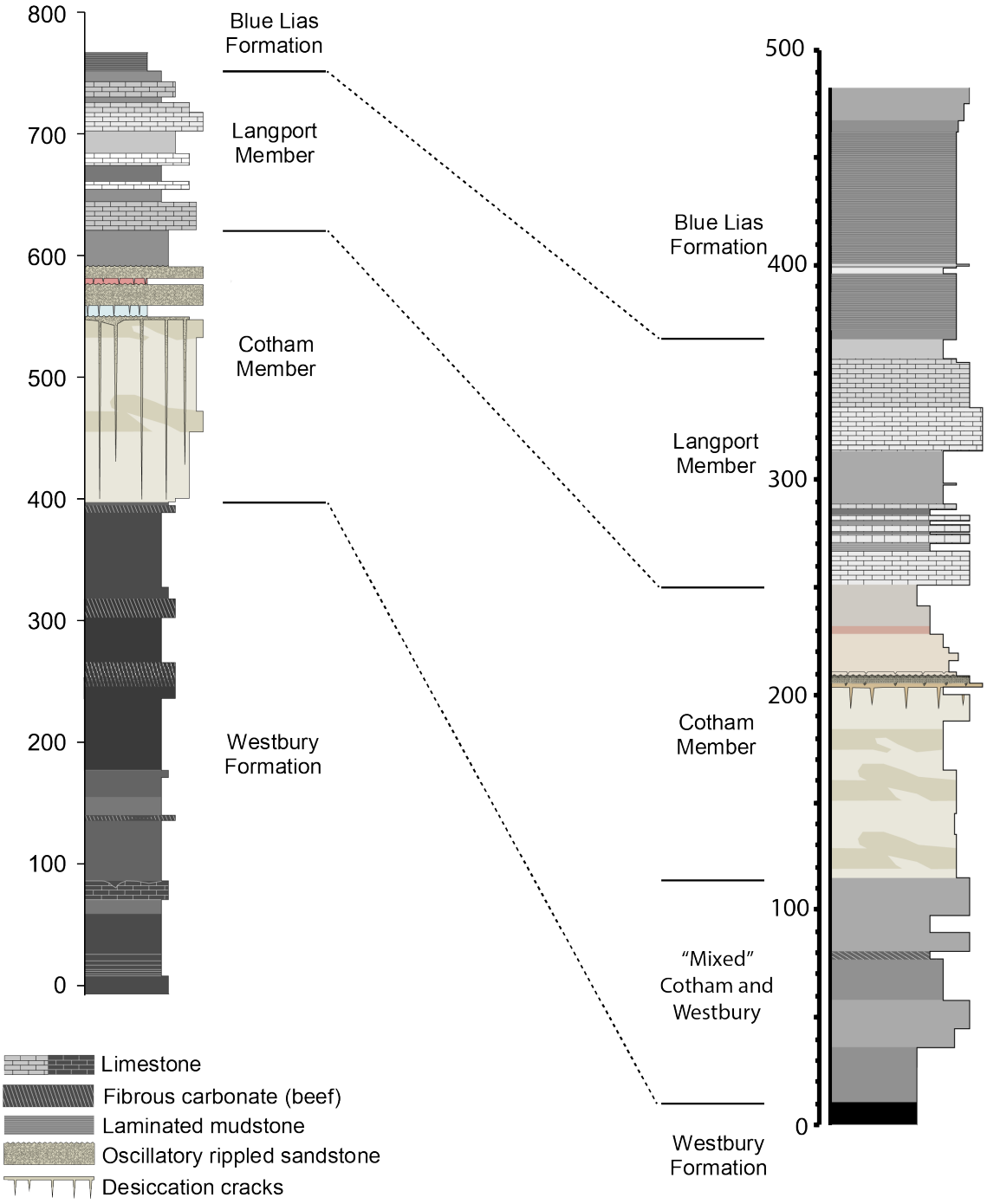


**Figure S1.** Lithology of and correlation between St. Audrie's Bay (left) and Lilstock (right).

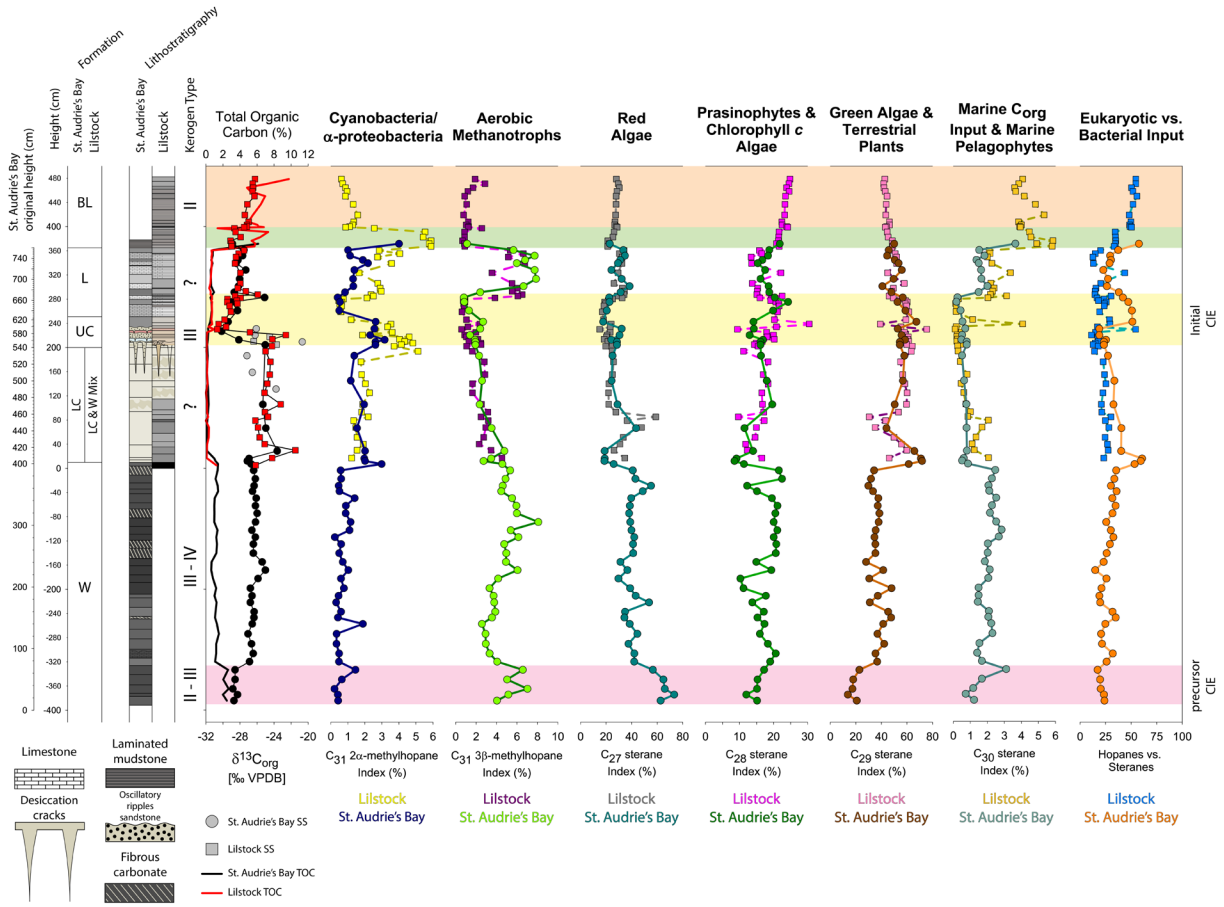


**Figure S2.** Biomarker inferred ecological changes at St. Audrie's Bay (circles and solid lines) and Lilstock (squares and dashed lined) relative to changes in the $\delta^{13}C_{org}$ and total organic carbon (TOC) records. The two depositional environments are indicated by the shaded green (PZE persisting through much of the photic zone) and shaded pink (PZE limited to lower depths in the photic zone) areas. Initial CIE and precursor CIE given in yellow and pink, respectively. Biomarker ratios and indices are given below and their ecological indicators given above each respective profile. Although this paper primarily focuses on the paper shales, we include full data here to show changes across the latest Rhaetian for completeness. For full details of biomarkers see Table DR1. Formation abbreviations: W – Westbury Formation; LC – Lower Cotham Member (Lilstock Formation); UC – Upper Cotham Member (Lilstock Formation); L – Langport Member (Lilstock Formation); BL – Blue Lias Formation; W – Westbury Formation. SS – Sandstone.

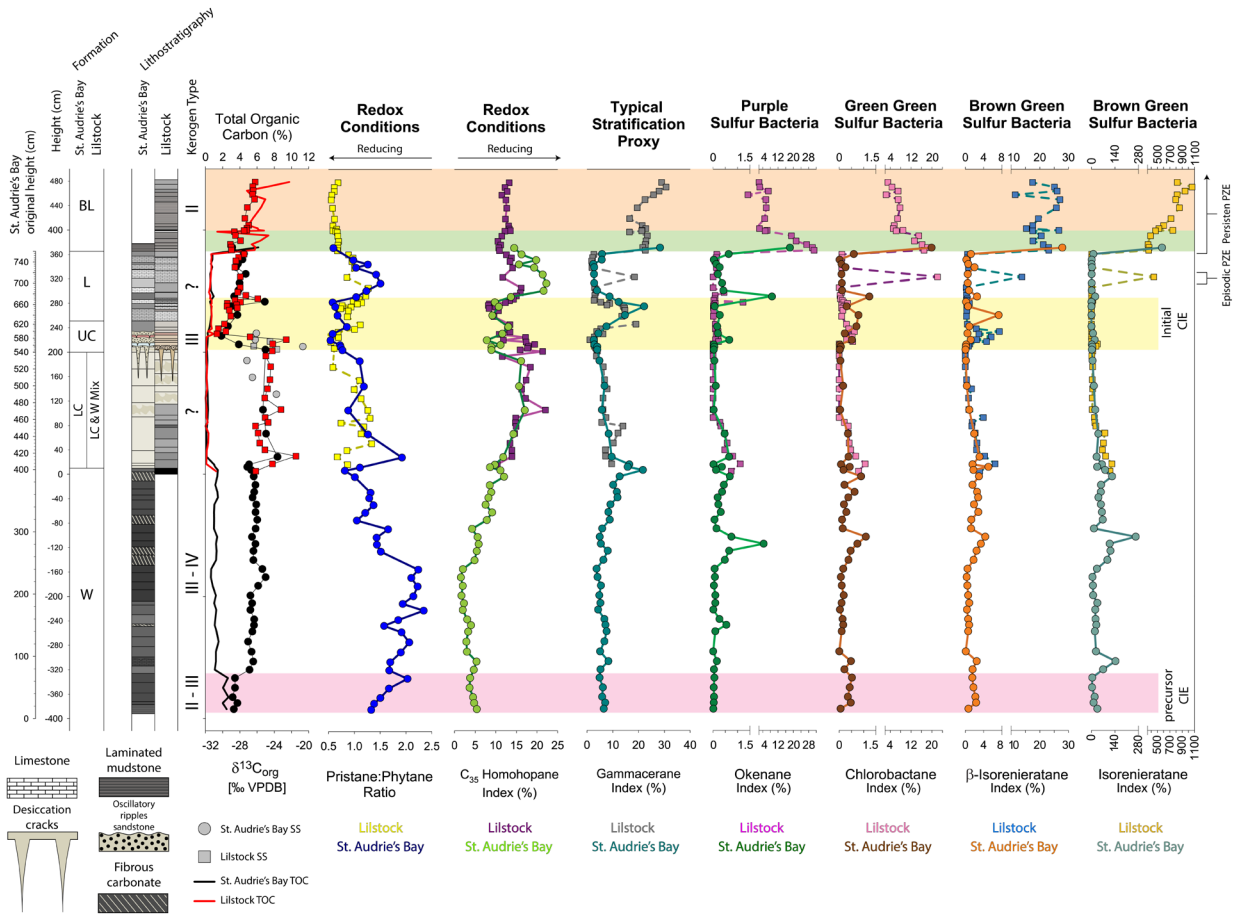


**Figure S3.** Biomarker inferred redox changes at St. Audrie's Bay (circles and solid lines) and Lilstock (squares and dashed lined) relative to changes in the $\delta^{13}C_{org}$ and total organic carbon (TOC) records. The two depositional environments are indicated by the shaded green (PZE persisting through much of the photic zone) and shaded pink (PZE limited to lower depths in the photic zone) areas. Initial CIE and precursor CIE given in yellow and pink, respectively. Biomarker ratios and indices are given below and their ecological indicators given above each respective profile. Although this paper primarily focuses on the paper shales, we include full data here to show changes across the latest Rhaetian for completeness. For full details of biomarkers see Table DR1. Formation abbreviations: W – Westbury Formation; LC – Lower Cotham Member (Lilstock Formation); UC – Upper Cotham Member (Lilstock Formation); L – Langport Member (Lilstock Formation); BL – Blue Lias Formation; W – Westbury Formation. SS – Sandstone

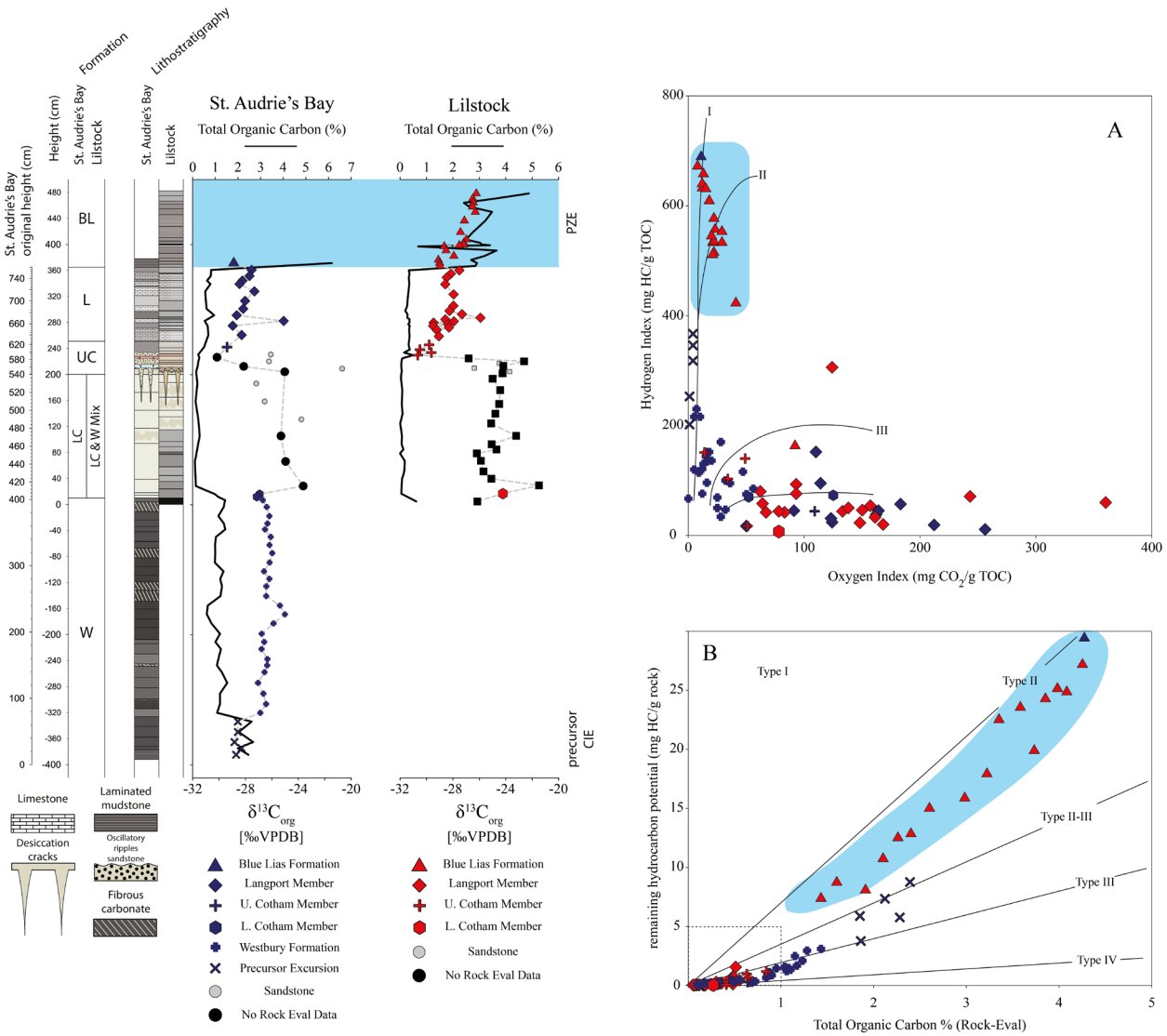


**Figure S4.** Left: St. Audrie's Bay and Lilstock total organic carbon (TOC) records and $\delta^{13}C_{org}$ changes with $\delta^{13}C_{org}$ symbols matching the Rock-Eval data. Blue shaded area indicates the paper shales. Although this paper primarily focuses on the paper shales, we include full data here to show changes across the latest Rhaetian. Formation abbreviations: W – Westbury Formation; LC – Lower Cotham Member; UC – Upper Cotham Member (Lilstock Formation); L – Langport Member (Lilstock Formation); BL – Blue Lias Formation. Right: Rock-Eval data with corresponding highlighted area as in left figure. A) Kerogen type by van Krevelen diagram. HC – hydrocarbon. B) kerogen type by relationship between remaining hydrocarbon potential and TOC. Dashed box indicates TOC lean samples.

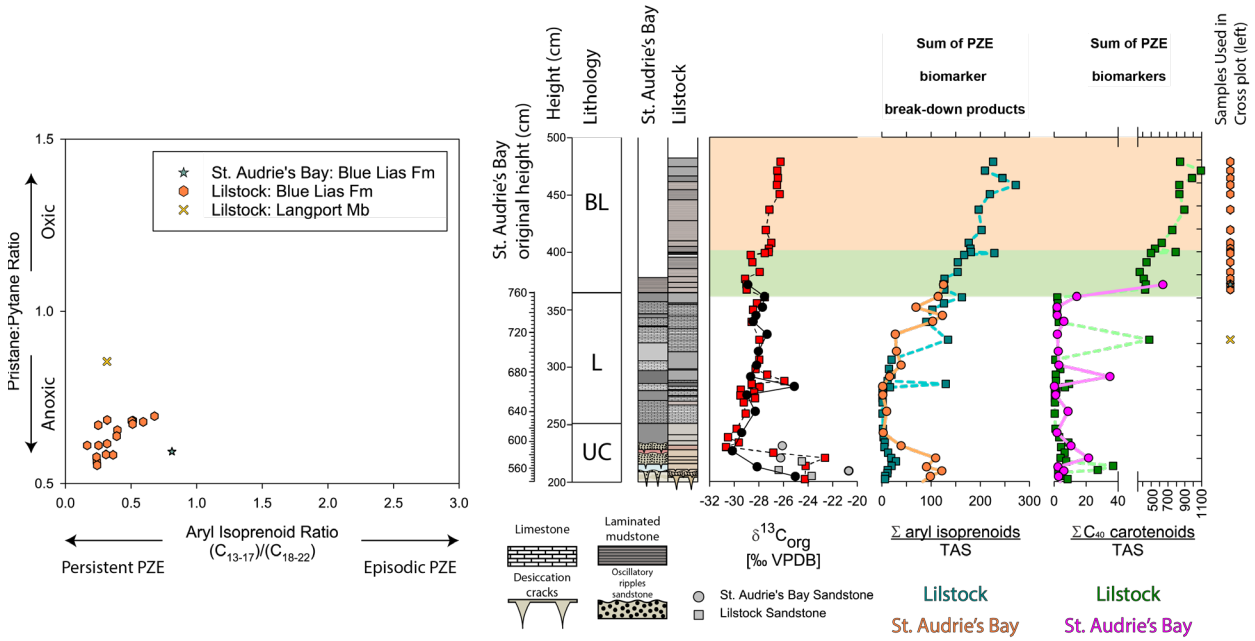


**Figure S5.** Left: Cross plot of the aryl isoprenoid ratio (AIR) and pristane to phytane ratio (Pr/Ph) through the different lithologies of the St. Audrie's Bay and Lilstock sections. Fm – Formation, Mb – Member. Right: Changes in the sum of aryl isoprenoids and sum of $C_{40}$ carotenoids (okenane, chlorobactane, β-isorenieratane, and isorenieratane) to triaromatic steroids (TAS) relative to the $\delta^{13}C_{org}$ record. The two depositional environments are indicated by the shaded green (PZE persisting through much of the photic zone) and shaded pink (PZE limited to lower depths in the photic zone) areas. BL – Blue Lias Formation, L - Langport Member, UC – upper Cotham Member.

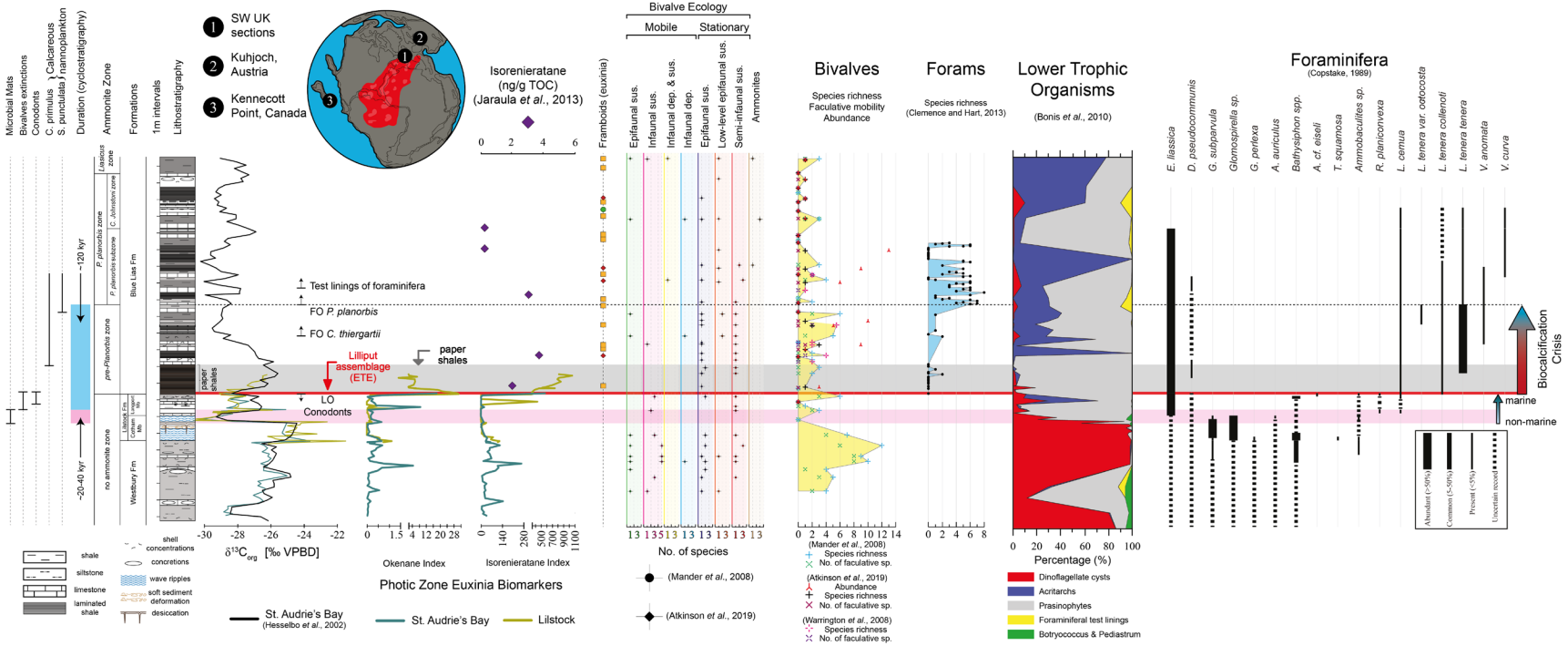
Microbial Mats
Bivalves extinctions
Conodonts
C. primulus
S. punctulata
Calcareous nannoplankton
Duration (cyclostratigraphy)
Ammonite Zone
Formations
1m intervals
Lithostratigraphy
1 SW UK sections
2 Kuhjoch, Austria
3 Kennecott Point, Canada
Isorenieratane (ng/g TOC) (Jaraula et al., 2013)
Framboids (euxinia)
Bivalve Ecology
Mobile
Stationary
Epifaunal sus.
Infaunal sus.
Infaunal dep. & sus.
Infaunal dep.
Epifaunal sus.
Low-level epifaunal sus.
Semi-infaunal sus.
Ammonites
Bivalves
Species richness
Facultative mobility
Abundance
Forams
Species richness
(Clemence and Hart, 2013)
Lower Trophic Organisms
(Bonis et al., 2010)
Foraminifera
(Copstake, 1989)
E. liassica
D. pseudocommunis
G. subparvula
Glomospirella sp.
G. perlexa
A. auriculus
Bathysiphon spp.
A. cf. eiseli
T. squamosa
Ammobaculites sp.
R. planiconvexa
L. cemua
L. tenera var. ootocosta
L. tenera collenoti
L. tenera tenera
V. anomata
V. curva
Lassicus zone
P. planorbis zone
C. Johnstoni zone
P. planorbis subzone
pre-Planorbis zone
no ammonite zone
Blue Lias Fm
Lilstock Fm
Cotham Member
Mb
Westbury Fm
~120 kyr
~20-40 kyr
paper shales
Test linings of foraminifera
FO P. planorbis
FO C. thiergartii
Lilliput assemblage (ETE)
LO Conodonts
Biocalcification Crisis
marine
non-marine
shale
siltstone
limestone
laminated shale
shell concentrations
concretions
wave ripples
soft sediment deformation
desiccation
δ13Corg [‰ VPBD]
St. Audrie's Bay (Hesselbo et al., 2002)
Okenane Index
Isorenieratane Index
St. Audrie's Bay
Lilstock
Photic Zone Euxinia Biomarkers
No. of species
(Mander et al., 2008)
(Atkinson et al., 2019)
(Mander et al., 2008)
Species richness
No. of faculative sp.
(Atkinson et al., 2019)
Abundance
Species richness
No. of faculative sp.
(Warrington et al., 2008)
Species richness
No. of faculative sp.
Percentage (%)
Dinoflagellate cysts
Acritarchs
Prasinophytes
Foraminiferal test linings
Botryococcus & Pediastrum
Abundant (>50%)
Common (5-50%)
Present (<5%)
Uncertain record

**Table S1.** Biomarker information including equations, MRM reactions, and typical precursors.

| Index/Biomarker | Calculation | MRM | Typical precursor |
|---|---|---|---|
| **Steranes** | | | |
| **$C_{27}$ Sterane Index (%) (all)** | $\frac{\sum C_{27}\text{Steranes}}{\sum C_{27-30}\text{Steranes}} \times 100$ | 372 → 217 | Red Algae (Patterson, 1971; Kodner et al., 2008) |
| **$C_{28}$ Sterane Index (%) (all)** | $\frac{\sum C_{28}\text{Steranes}}{\sum C_{27-30}\text{ Steranes}} \times 100$ | 386 → 217 | Chlorophyll *c* algae and prasinophytes (Volkman et al., 1994, 1998) |
| **$C_{29}$ Sterane Index (%) (all)** | $\frac{\sum C_{29}\text{ Steranes}}{\sum C_{27-30}\text{Steranes}} \times 100$ | 400 → 217 | Green algae and/or terrestrial plants (Volkman et al., 1994; Kodner et al., 2008) |
| **$C_{30}$ Sterane Index (%) (diasteranes)** | $\frac{\sum C_{30}\text{ Diasteranes}}{\sum C_{27-30}\text{Diateranes}} \times 100$ | 414 → 217 | Marine algae (Peters et al., 2004) |
| **Hopanes** | | | |
| **$C_{31}$ 2α-methylhopane Index (%)** | $\frac{C_{31}2\alpha\text{ Methylhopane}}{C_{30}\alpha\beta\text{ Hopane}} \times 100$ | 426 → 205 | Aerobic cyanobacteria (Summons et al., 1999), α-proteobacteria (Rashby et al., 2007; Ricci et al., 2015), shifts in environment (Ricci et al., 2014 and references therein), ecological stress (Ricci et al., 2017), nitrite-oxidizing bacteria (Elling et al., 2020) |
| **$C_{31}$ 3β-Methylhopane Index (%)** | $\frac{C_{31}3\beta\text{ Methylhopane}}{C_{30}\alpha\beta\text{ Hopane}} \times 100$ | 426 → 205 | Aerobic methanotrophs (Rohmer et al., 1984; Summons and Jahnke, 1990) |
| **Gammacerane Index (%)** | $\frac{C_{30}\text{ Gammacerane}}{C_{30}\alpha\beta\text{ Hopane}} \times 100$ | 412 → 191 | Stratification (Sinninghe Damsté et al., 1995) |
| **$C_{40}$ Carotenoids** | | | |
| **Okenane Index** | $\frac{Okenane}{\sum C_{26-28}TAS} \times 1000$ | 554 → 134 | Chromatiaceae (Schaeffer et al., 1997; Brocks and Schaeffer, 2008) |
| **Chlorobactane Index** | $\frac{Chlorobactane}{\sum C_{26-28}TAS} \times 1000$ | 554 → 134 | Green-pigmented Chlorobiaceae (Grice et al., 1998) |
| **β-Isorenieratane Index** | $\frac{\beta - isorenieratane}{\sum C_{26-28}TAS} \times 1000$ | 552 → 134 | Brown-pigmented Chlorobiaceae (Grice et al., 1998) |
| **Isorenieratane Index** | $\frac{Isorenieratane}{\sum C_{26-28}TAS} \times 1000$ | 546 → 134 | Brown-pigmented Chlorobiaceae (Jensen, 1965; Summons and Powell, 1986; Grice et al., 1996) |
| ***n*-alkanes** | | | |
| **$C_{17}$ *n*-alkane** | For CSIA | (run on GC-MS and GC-IRMS) | Photosynthetic bacteria and algae (Cranwell et al., 1987) |
| **$C_{18}$ *n*-alkane** | | | |
| **$C_{19}$ *n*-alkane** | | | |
| **$C_{29}$ *n*-alkane** | For CSIA | (run on GC-MS and GC-IRMS) | Land plants (Eglinton et al., 1962) |
| **Others** | | | |
| **Pristane to Phytane Ratio** | $\frac{Pristane}{Phytane}$ | Identified using GC-MS | Redox conditions (Powell and McKirdy, 1973; Didyk et al., 1978) |
| **Hopanes Vs. Steranes Index (%)** | $\frac{C_{27-30}\ Steranes\ (reg)}{C_{27-35}\ Hopanes + C_{27-30}\ Steranes\ (reg)}$ | See above | Eukaryotic vs. bacterial input (Peters et al., 2004) |

**Table S2.** Rock-Eval pyrolysis data from St. Audrie's Bay and Lilstock.

| St. Audrie's Bay | | | | | | | | | | | | | | | |
|---|---|---|---|---|---|---|---|---|---|---|---|---|---|---|---|
| TOC (%) | | S1 | | S2 | | S3 | | PI | | HI | | OI | | Tmax (°C) | |
| Min | 0.06 | Min | 0 | Min | 0.01 | Min | 0 | Min | 0 | Min | 11 | Min | 0 | Min | 421 |
| Max | 2.39 | Max | 0.12 | Max | 8.79 | Max | 0.7 | Max | 0.12 | Max | 367 | Max | 256 | Max | 435 |
| Lilstock | | | | | | | | | | | | | | | |
| TOC (%) | | S1 | | S2 | | S3 | | PI | | HI | | OI | | Tmax (°C) | |
| Min | 0.05 | Min | 0 | Min | 0.02 | Min | 0.07 | Min | 0.01 | Min | 7 | Min | 8 | Min | 418 |
| Max | 4.25 | Max | 1.17 | Max | 27.18 | Max | 0.86 | Max | 0.14 | Max | 627 | Max | 360 | Max | 433 |

TOC – Total Organic Carbon (wt%)

S1 – Volatile hydrocarbon (HC) content (mg HC/mg rock)

S2 – Remaining HC generative potential (mg HC/mg rock)

S3 – $CO_2$ content (mg $CO_2$/mg rock)

Production Index (PI) – S1/(S1+S2)

Hydrogen Index (HI) – (S2*100)/TOC

Oxygen Index (OI) – (S3*100)/TOC, mg $CO_2$/g TOC

**Table S3.** Bivalves of the lower Blue Lias Formation in St. Audrie's Bay and their ecology. Those that are facultative in their mobility are indicated by asterisks.

| **Mobile** | | |
|---|---|---|
| **Epifaunal Suspension Feeder** | | |
| **Bivalve** | **Reported by** | **Reference** |
| *Chlamys Valoneinsis** | Mander et al., (2008) | (Johnson, 1984) |
| *Pseudomytiloides dubius** | Mander et al., (2008) | (Ros-Franch et al., 2015) |
| **Infaunal Suspension Feeder** | | |
| **Bivalve** | **Reported by** | **Reference** |
| *Cardinia regularis** | Mander et al., (2008) | (Ros-Franch et al., 2014) |
| *Isocyprina sp.** | Mander et al., (2008) | (Ros-Franch et al., 2014) |
| *Isocyprina concentricum** | Mander et al., (2008) | (Ros-Franch et al., 2014) |
| *Isocyprina ewaldi** | Mander et al., (2008) | (Márquez-Aliaga et al., 2010; Ros-Franch et al., 2014) |
| *Lyriomyophoria postera** | Mander et al., (2008) | (Friesenbichler et al.; Ros-Franch et al., 2014) |
| *Permophorus elongtus** | Mander et al., (2008) | (Mendes, 1952; Foster et al., 2019) |
| *Pleuromya sp.** | Mander et al., (2008) | (Aberhan, 2004; Ros-Franch et al., 2014) |
| *Prorocardia philippianum* | Atkinson and Wignal (2019) | (Ros-Franch et al., 2014) |
| *Protocardia rhaetica** | Mander et al., (2008) | (Ros-Franch et al., 2014) |
| *Pteromya crowcombia** | Mander et al., (2008) | (Márquez-Aliaga et al., 2010; Ros-Franch et al., 2014) |
| *Tutcheria cloacina** | Mander et al., (2008) | (Márquez-Aliaga et al., 2010; Ros-Franch et al., 2014) |
| **Infaunal Deposit & Suspension Feeder** | | |
| **Bivalve** | **Reported by** | **Reference** |
| *Palaeonucula navis** | Mander et al., (2008) | (Chen, 1982; Hodges, 2000) |
| **Infaunal Deposit Feeder** | | |
| **Bivalve** | **Reported by** | **Reference** |
| *Ryderia sp.** | Mander et al., (2008) | (Yin and McRoberts, 2006) |
| *Rollieria bronni** | Mander et al., (2008) | (Ros-Franch et al., 2014) |
| **Stationary** | | |
| **Epifaunal Suspension Feeder** | | |
| **Bivalve** | **Reported by** | **Reference** |
| *Anningella cf. faberi* | Atkinson and Wignal (2019) | (Ros-Franch et al., 2014) |
| *Cassianella sp.* | Mander et al., (2008) | (Nützel and Kaim, 2014; Ros-Franch et al., 2014) |
| *Chlamys textoria* | Atkinson and Wignal (2019) | (Johnson, 1984; Damborenea, 2002) |
| *Liostrea spp.* | Mander et al., (2008) and Atkinson and Wignal (2019) | (Ros-Franch et al., 2014) |
| *Liostrea bristovi* | Mander et al., (2008) | (Ros-Franch et al., 2014) |
| *Liostrea hisingeri* | Mander et al., (2008) | (Ros-Franch et al., 2014) |
| *Mytilus cloacinus* | Mander et al., (2008) | (Tutcher, 1908) |
| *Oxytoma fallax* | Mander et al., (2008) | (Ros-Franch et al., 2014) |
| *Placunopsis alpina* | Mander et al., (2008) | (Márquez-Aliaga et al., 2010) |

| | | |
|---|---|---|
| *Pseudolimea pectinoids* | Atkinson and Wignal (2019) | (Szente, 1992; Damborenea and Mancenido, 2005) |
| *Rhaetavicula contorta* | Mander et al., (2008) | (MacFadyen, 1970) |
| **Low-Level Epifaunal Suspension Feeder** | | |
| **Bivalve** | **Reported by** | **Reference** |
| *Plagiostoma giganteum* | Mander et al., (2008) and Atkinson and Wignal (2019) | (Yin and McRoberts, 2006) |
| *Plagiostoma punctatum* | Mander et al., (2008) | (Paredes et al., 2013) |
| **Semi-Infaunal Suspension Feeder** | | |
| **Bivalve** | **Reported by** | **Reference** |
| *Gervillella ornata* | Mander et al., (2008) | (Ros-Franch et al., 2014; Foster et al., 2019) |
| *Modiolus spp.* | Mander et al., (2008) | (Hodges, 2000; Márquez-Aliaga et al., 2010; Paredes et al., 2013) |
| *Modiolus hillanus* | Mander et al., (2008) | (Hodges, 2000; Paredes et al., 2013) |
| *Modiolus minimus* | Mander et al., (2008) and Atkinson and Wignal (2019) | (Hodges, 2000; Márquez-Aliaga et al., 2010) |
| *Modiolus sodburiensis* | Mander et al., (2008) | (Hodges, 2000; Márquez-Aliaga et al., 2010; Paredes et al., 2013) |

## References


Aberhan, M., 2004, Early Jurassic Bivalvia of northern Chile. Part II. Subclass Anomalodesmata: Beringeria, v. 34, p. 117–154.

Atkinson, J.W., and Wignall, P.B., 2019, How quick was marine recovery after the end-Triassic mass extinction and what role did anoxia play? Palaeogeography, Palaeoclimatology, Palaeoecology, v. 528, p. 99–119, doi:10.1016/j.palaeo.2019.05.011.

Behar, F., Beaumont, V., and De B. Penteado, H.L., 2001, Rock-Eval 6 Technology: Performances and Developments: Oil & Gas Science and Technology, v. 56, p. 111–134, doi:10.2516/ogst:2001013.

Brocks, J.J., and Schaeffer, P., 2008, Okenane, a biomarker for purple sulfur bacteria (Chromatiaceae), and other new carotenoid derivatives from the 1640 Ma Barney Creek Formation: Geochimica et Cosmochimica Acta, v. 72, p. 1396–1414, doi:10.1016/j.gca.2007.12.006.

Chen, J.H., 1982, Liassic bivalve fossils from Mount Jinji of Guangdong: Acta Palaeontologica Sinica, v. 21, p. 404–416.

Cranwell, P.A., Eglinton, G., and Robinson, N., 1987, Lipids of aquatic organisms as potential contributors to lacustrine sediments -II*: Organic geochemisy, v. 11, p. 513–527, doi:10.1016/0146-6380(87)90007-6.

Damborenea, S.E., 2002, Early Jurassic bivalves of Argentina Part 3: Superfamilies Monotoidea, Pectinoidea, Plicatuloidea and Dimyoidea: Palaeontographica, Abteilung A: Palaozoologie - Stratigraphie, v. 265, p. 1–119.

Damborenea, S.E., and Mancenido, M.O., 2005, Biofacies analysis of Hettangian-Sinemurian bivalve / brachiopod associations from the Neuquén Basin (Argentina): Geologica Acta, v. 3, p. 163–178, doi:https://doi.org/10.1344/105.000001405.

Didyk, B.M., Simoneit, B.R.T., Brassell, S.C., and Eglinton, G., 1978, Organic geochemical indicators of palaeoenvironmental conditions of sedimentation: Nature, v. 272, p. 216–222, doi:10.1038/272216a0.

Eglinton, G., Gonzalez, A.G., Hamilton, R.J., and Raphael, R.A., 1962, Hydrocarbon constituents of the wax coatings of plant leaves: A taxonomic Survey: Phytochemistry, v. 1, p. 89–102.

Foster, W.J., Lehrmann, D.J., Hirtz, J.A., White, M., Yu, M., Li, J., and Martindale, R.C., 2019, Early Triassic benthic invertebrates from the Great Bank of Guizhou, South China: systematic palaeontology and palaeobiology: Papers in Palaeontology, v. 5, p. 613–656, doi:10.1002/spp2.1252.

Fox, C.P., Cui, X., Whiteside, J.H., Olsen, P.E., Summons, R.E., and Grice, K., 2020, Molecular and isotopic evidence reveals the end-Triassic carbon isotope excursion is not from massive exogenous light carbon: Proceedings of the National Academy of Sciences, v. 117, p. 30171–30178, doi:10.1073/pnas.1917661117.

Friesenbichler, E., Hautmann, M., Grădinaru, E., and Bucher, H. A highly diverse bivalve fauna

from a Bithynian (Anisian, Middle Triassic) Tubiphytes-microbial buildup in North Dobrogea (Romania): Papers in Palaeontology, p. 1–49, doi:https://doi.org/10.1002/spp2.1286.

Grice, K., Schaeffer, P., Schwark, L., and Maxwell, J.R., 1996, Molecular indicators of palaeoenvironmental conditions in an immature Permian shale (Kupferschiefer, Lower Rhine Basin, north-west Germany) from free and S-bound lipids: Organic Geochemistry, v. 25, p. 131–147, doi:10.1016/S0146-6380(96)00130-1.

Grice, K., Schouten, S., Peters, K.E., and Sinninghe Damsté, J.S., 1998, Molecular isotopic characterisation of hydrocarbon biomarkers in Palaeocene-Eocene evaporitic, lacustrine source rocks from the Jianghan Basin, China: Organic Geochemistry, v. 29, p. 1745–1764, doi:10.1016/S0146-6380(98)00075-8.

Hesselbo, S.P., Robinson, S.A., Surlyk, F., and Piasecki, S., 2002, Terrestrial and marine extinction at the Triassic-Jurassic boundary synchronized with major carbon-cycle perturbation: A link to initiation of massive volcanism? Geology, v. 30, p. 251–254, doi:10.1130/0091-7613(2002)030<0251:TAMEAT>2.0.CO;2.

Hodges, P., 2000, The early Jurassic bivalvia from the Hettangian and lower Sinemurian of south-west Britain Part 1 (W. A. Rushton & A. T. Thomas, Eds.):

Jaraula, C.M.B., Grice, K., Twitchett, R.J., Böttcher, M.E., LeMetayer, P., Dastidar, A.G., and Opazo, L.F., 2013, Elevated $pCO_2$ leading to late triassic extinction, persistent photic zone euxinia, and rising sea levels: Geology, v. 41, p. 955–958, doi:10.1130/G34183.1.

Jensen, S.L., 1965, Bacterial Carotenoids XVIII Aryl-carotenese from phaeobium: Acta Chemica Scandinavica, v. 19, p. 1025–1030, doi:10.3891/acta.chem.scand.19-1025.

Johnson, A., 1984, The palaeobiology of the bivalve families Pectinidae and Propeamussiidae in the Jurassic of Europe: Zitteliana, v. 11, p. 3–235.

Kodner, R.B., Pearson, A., Summons, R.E., and Knoll, A.H., 2008, Sterols in red and green algae: Quantification, phylogeny, and relevance for the interpretation of geologic steranes: Geobiology, v. 6, p. 411–420, doi:10.1111/j.1472-4669.2008.00167.x.

MacFadyen, W.A., 1970, Geological highlights of the West Country: David and Charles, Newton Abbot, Devon, 1–296 p.

Mander, L., Twitchett, R.J., and Benton, M.J., 2008, Palaeoecology of the Late Triassic extinction event in the SW UK: Journal of the Geological Society, v. 165, p. 319–332, doi:10.1144/0016-76492007-029.

Márquez-Aliaga, A., Damborenea, S., Gómez, J.J., and Goy, A., 2010, Bivalves from the Triassic-Jurassic transition in northern Spain (Asturias and western Basque-Cantabrian Basin): Ameghiniana, v. 47, p. 185–205, doi:10.5710/AMGH.v47i2.3.

Mendes, J.C., 1952, A Formação Corumbataí na região do rio Corumbataí. (Estratigrafia e descrição dos lamelibrãnquios): Boletim da Faculdade de Filosofia Ciências e Letras, Universidade de São Paulo. Geologia, p. 5–127, doi:10.11606/issn.2526-3862.bffcluspgeologia.1952.128536.

Nützel, A., and Kaim, A., 2014, Diversity, palaeoecology and systematics of a marine fossil

assemblage from the Late Triassic Cassian Formation at Settsass Scharte, N Italy: Palaontologische Zeitschrift, v. 88, p. 405–431, doi:10.1007/s12542-013-0205-1.

Paredes, R., Comas-Rengifo, M.J., and Duarte, L. V., 2013, Moluscos bivalves da Formação de Água de Madeiros (Sinemuriano superior) da Bacia Lusitânica (Portugal): Comunicacoes Geologicas, v. 100, p. 21–27.

Patterson, G.W., 1971, The Distribution of Sterols in Algae: Lipids, v. 6, p. 120–127, doi:10.1097/NCQ.0000000000000180.

Peters, K.E., Walters, C.C., and Moldowan, J.M., 2004, The Biomarker Guide: Volume 2: Biomarkers and Isotopes in Petroleum Systems and Earth History: Cambridge, Cambridge University Press, v. 2, doi:DOI: 10.1017/CBO9781107326040.

Powell, T.G., and McKirdy, D.M., 1973, Relationship between ratio of pristane to phytane, crude oil composition and geological environment in Australia: Nature, v. 243, p. 37–39, doi:10.1038/246421a0.

Rashby, S.E., Sessions, A.L., Summons, R.E., and Newman, D.K., 2007, Biosynthesis of 2-methylbacteriohopanepolyols by an anoxygenic phototroph: Proceedings of the National Academy of Sciences, v. 104, p. 15099–15104, doi:10.1073/pnas.0704912104.

Ricci, J.N., Coleman, M.L., Welander, P. V., Sessions, A.L., Summons, R.E., Spear, J.R., and Newman, D.K., 2014, Diverse capacity for 2-methylhopanoid production correlates with a specific ecological niche: ISME Journal, v. 8, p. 675–684, doi:10.1038/ismej.2013.191.

Ricci, J.N., Michel, A.J., and Newman, D.K., 2015, Phylogenetic analysis of HpnP reveals the origin of 2-methylhopanoid production in Alphaproteobacteria: Geobiology, v. 13, p. 267–277, doi:10.1111/gbi.12129.

Ricci, J.N., Morton, R., Kulkarni, G., Summers, M.L., and Newman, D.K., 2017, Hopanoids play a role in stress tolerance and nutrient storage in the cyanobacterium Nostoc punctiforme: Geobiology, v. 15, p. 173–183, doi:10.1111/gbi.12204.

Rohmer, M., Bouvier-Nave, P., and Ourisson, G., 1984, Distribution of hopanoid triterpenes in prokaryotes: Microbiology, v. 130, p. 1137–1150, doi:10.1099/00221287-130-5-1137.

Ros-Franch, S., Damborenea, S.E., Márquez-Aliaga, A., and Manceñido, M.O., 2015, Parainoceramya n. Gen. For Parainoceramus Cox, 1954 (ex Voronetz, 1936) Partim (Bivalvia, Jurassic): Journal of Paleontology, v. 89, p. 20–27, doi:10.1017/jpa.2014.3.

Ros-Franch, S., Marquez-Aliaga, A., and Damborenea, S.E., 2014, Comprehensive database on Induan (Lower Triassic) to Sinemurian (Lower Jurassic) marine bivalve genera and their paleobiogeographic record: Paleontological Contributions, v. 8, p. 1–129, doi:10.17161/pc.1808.13433.

Schaeffer, P., Adam, P., Wehrung, P., and Albrecht, P., 1997, Novel aromatic carotenoid derivatives from sulfur photosynthetic bacteria in sediments: Tetrahedron Letters, doi:10.1016/S0040-4039(97)10235-0.

van de Schootbrugge, B., Tremolada, F., Rosenthal, Y., Bailey, T.R., Feist-Burkhardt, S., Brinkhuis, H., Pross, J., Kent, D. V., and Falkowski, P.G., 2007, End-Triassic calcification crisis and blooms of organic-walled “disaster species”: Palaeogeography,

Palaeoclimatology, Palaeoecology, v. 244, p. 126–141, doi:10.1016/j.palaeo.2006.06.026.
Schwark, L., and Frimmel, A., 2004, Chemostratigraphy of the Posidonia Black Shale, SW-Germany II. Assessment of extent and persistence of photic-zone anoxia using aryl isoprenoid distributions: Chemical Geology, v. 206, p. 231–248, doi:10.1016/j.chemgeo.2003.12.008.
Sinninghe Damsté, J.S., Kenig, F., Koopmans, M.P., Köster, J., Schouten, S., Hayes, J.M., and de Leeuw, J.W., 1995, Evidence for gammacerane as an indicator of water column stratification: Geochimica et Cosmochimica Acta, v. 59, p. 1895–1900, doi:10.1016/0016-7037(95)00073-9.
Skrzypek, G., 2013, Normalization procedures and reference material selection in stable HCNOS isotope analyses: An overview: Analytical and Bioanalytical Chemistry, v. 405, p. 2815–2823, doi:10.1007/s00216-012-6517-2.
Skrzypek, G., and Debajyoti, P., 2006, $\delta^{13}C$ analyses of calcium carbonate: comparison between the GasBench and elemental analyzer techniques Grzegorz: Rapid Communications in Mass Spectrometry, v. 20, p. 2915–2920, doi:10.1002/rcm.
Summons, R.E., and Jahnke, L.L., 1990, Identification of the methylhopanes in sediments and petroleum: Geochimica et Cosmochimica Acta, v. 54, p. 247–251, doi:10.1016/0016-7037(90)90212-4.
Summons, R.E., Jahnke, L.L., Hope, J.M., and Logan, G.A., 1999, 2-Methylhopanoids as biomarkers for cyanobacterial oxygenic photosynthesis.: Nature, v. 400, p. 554–557, doi:10.1038/23005.
Summons, R.E., and Powell, T.G., 1986, Chlorobiaceae in Palaeozoic seas revealed by biological markers, isotopes and geology: Nature, v. 319, p. 763–765, doi:10.1038/319763a0.
Swift, A., 1989, First records of conodonts from the Late Triassic of Britain: Palaeontology, v. 32, p. 325–333.
Szente, I., 1992, A Pliensbachian (early Jurassic) bivalve faunula from the Harsány-hegy: First record of the Domerian substage from the Villány Hills (southern Hungary): Fragmenta Mineralogica et Palaeontologica, v. 15, p. 95–106.
Tutcher, J.W., 1908, The strata exposed in constructing the Filton to Avonmouth Railway: Bristol Proceedings Naturalists Society, v. 2, p. 5–21.
Volkman, J.K., Barrett, S.M., Blackburn, S.I., Mansour, M.P., Sikes, E.L., and Gelin, F., 1998, Microalgal biomarkers: A review of recent research developments: Organic Geochemistry, v. 29, p. 1163–1179, doi:10.1016/S0146-6380(98)00062-X.
Volkman, J.K., Barrett, S.M., Dunstan, G.A., and Jeffrey, S.W., 1994, Sterol biomarkers for microalgae from the green algal class Prasinophyceae: Organic Geochemistry, v. 21, p. 1211–1218, doi:10.1016/0146-6380(94)90164-3.
Whiteside, J.H., Olsen, P.E., Eglinton, T., Brookfield, M.E., and Sambrotto, R.N., 2010, Compound-specific carbon isotopes from Earth's largest flood basalt eruptions directly linked to the end-Triassic mass extinction: Proceedings of the National Academy of

Sciences of the United States of America, v. 107, p. 6721–6725, doi:10.1073/pnas.1001706107.

Wilkin, R.T., Barnes, H.L., and Brantley, S.L., 1996, The size distribution of framboidal pyrite in modern sediments: An indicator of redox conditions: Geochimica et Cosmochimica Acta, v. 60, p. 3897–3912, doi:10.1016/0016-7037(96)00209-8.

Yin, J., and McRoberts, C.A., 2006, Latest Triassic–earliest Jurassic bivalves of the Germig formation from Lanongla: Journal of Paleontology, v. 80, p. 104–120, doi:10.1666/0022-3360(2006)080[0104:ltjbot]2.0.co;2.

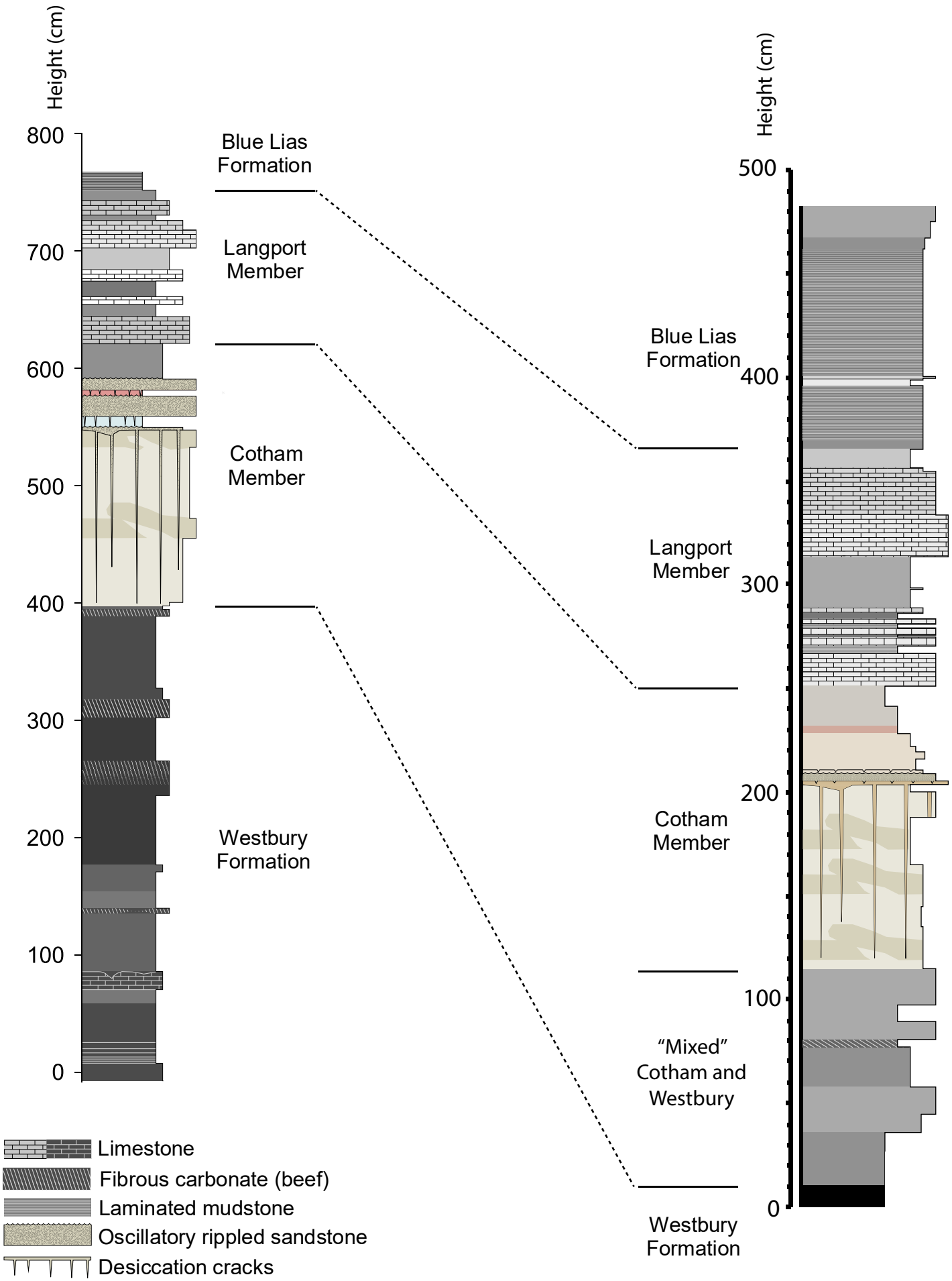
Height (cm)
800
700
600
500
400
300
200
100
0
Blue Lias Formation
Langport Member
Cotham Member
Westbury Formation
Height (cm)
500
400
300
200
100
0
Blue Lias Formation
Langport Member
Cotham Member
"Mixed" Cotham and Westbury
Westbury Formation
Limestone
Fibrous carbonate (beef)
Laminated mudstone
Oscillatory rippled sandstone
Desiccation cracks

Fig. S1

Fig. S2

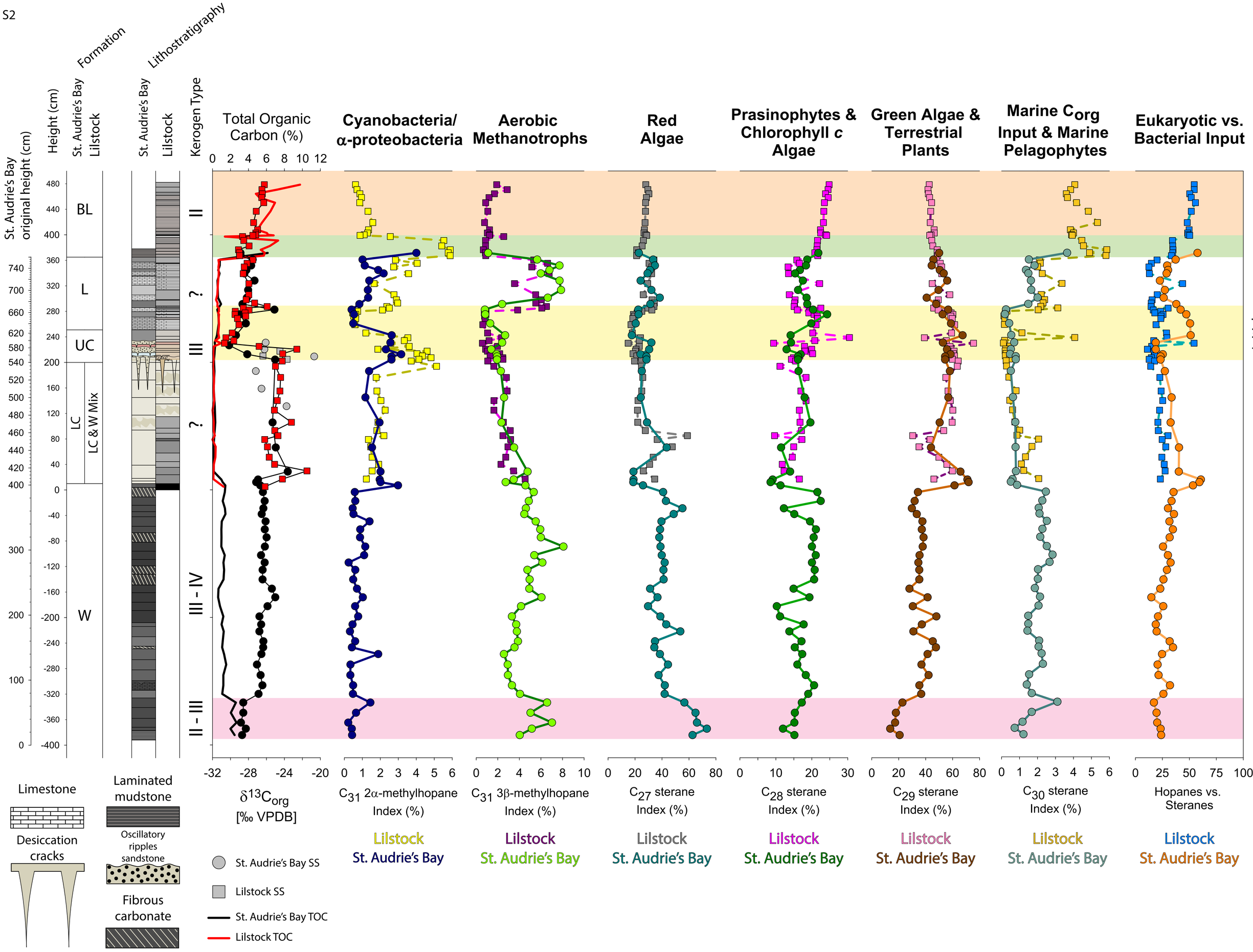
Formation
Lithostratigraphy
St. Audrie's Bay original height (cm)
Height (cm)
St. Audrie's Bay
Lilstock
St. Audrie's Bay
Lilstock
Kerogen Type
Total Organic Carbon (%)
0 2 4 6 8 10 12
Cyanobacteria/ α-proteobacteria
Aerobic Methanotrophs
Red Algae
Prasinophytes & Chlorophyll c Algae
Green Algae & Terrestrial Plants
Marine Corg Input & Marine Pelagophytes
Eukaryotic vs. Bacterial Input
BL
L
UC
LC
LC & W Mix
W
II
?
III
?
III - IV
II - III
Initial CIE
precursor CIE
Limestone
Desiccation cracks
Laminated mudstone
Oscillatory ripples sandstone
Fibrous carbonate
St. Audrie's Bay SS
Lilstock SS
St. Audrie's Bay TOC
Lilstock TOC
δ13Corg [‰ VPDB]
C31 2α-methylhopane Index (%)
C31 3β-methylhopane Index (%)
C27 sterane Index (%)
C28 sterane Index (%)
C29 sterane Index (%)
C30 sterane Index (%)
Hopanes vs. Steranes
Lilstock
St. Audrie's Bay

Fig. S3

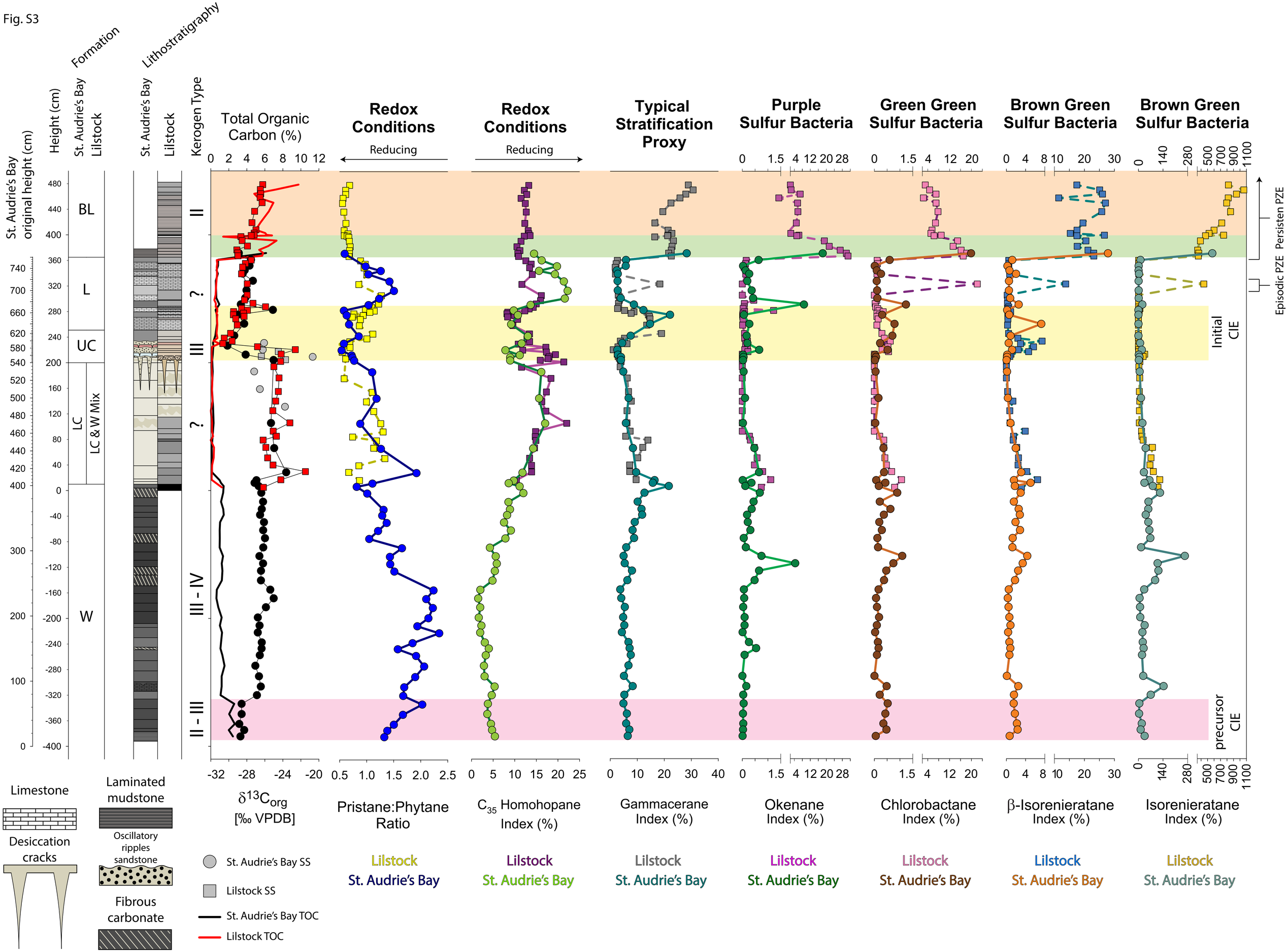
Formation
Lithostratigraphy
St. Audrie's Bay original height (cm)
Height (cm)
St. Audrie's Bay
Lilstock
Kerogen Type
Total Organic Carbon (%)
Redox Conditions
Reducing
Redox Conditions
Reducing
Typical Stratification Proxy
Purple Sulfur Bacteria
Green Green Sulfur Bacteria
Brown Green Sulfur Bacteria
Brown Green Sulfur Bacteria
BL
L
UC
LC
LC & W Mix
W
II
?
III
?
III - IV
II - III
Initial CIE
precursor CIE
Episodic PZE
Persisten PZE
Limestone
Desiccation cracks
Laminated mudstone
Oscillatory ripples sandstone
Fibrous carbonate
St. Audrie's Bay SS
Lilstock SS
St. Audrie's Bay TOC
Lilstock TOC
δ13Corg [‰ VPDB]
Pristane:Phytane Ratio
C35 Homohopane Index (%)
Gammacerane Index (%)
Okenane Index (%)
Chlorobactane Index (%)
β-Isorenieratane Index (%)
Isorenieratane Index (%)
Lilstock
St. Audrie's Bay

Fig. S4

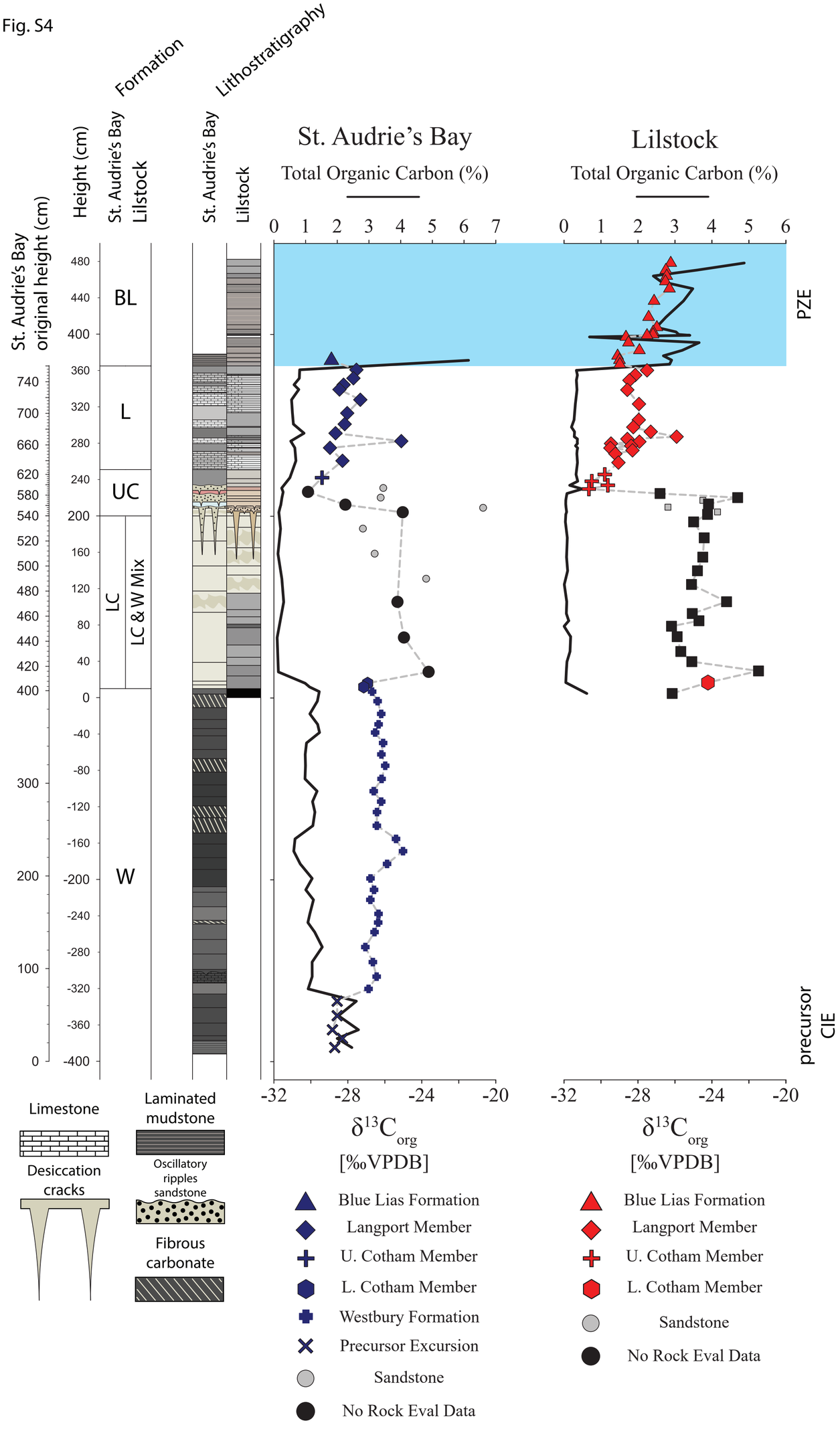
Formation
Lithostratigraphy
St. Audrie's Bay original height (cm)
Height (cm)
St. Audrie's Bay
Lilstock
St. Audrie's Bay
Lilstock
St. Audrie's Bay
Total Organic Carbon (%)
Lilstock
Total Organic Carbon (%)
PZE
precursor CIE
BL
L
UC
LC
LC & W Mix
W
Limestone
Laminated mudstone
Desiccation cracks
Oscillatory ripples sandstone
Fibrous carbonate
δ13Corg [‰VPDB]
δ13Corg [‰VPDB]
Blue Lias Formation
Langport Member
U. Cotham Member
L. Cotham Member
Westbury Formation
Precursor Excursion
Sandstone
No Rock Eval Data
Blue Lias Formation
Langport Member
U. Cotham Member
L. Cotham Member
Sandstone
No Rock Eval Data

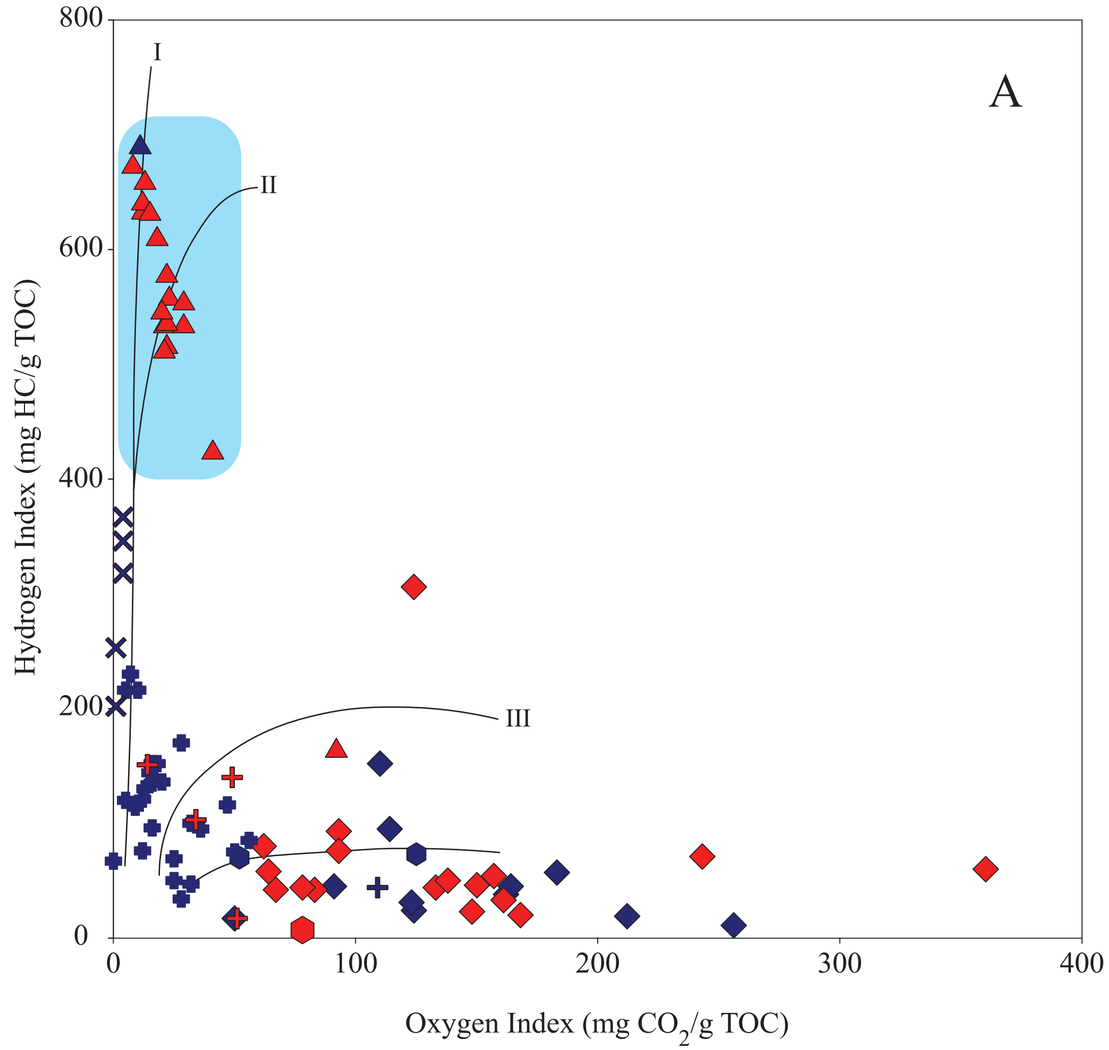
A
Hydrogen Index (mg HC/g TOC)
Oxygen Index (mg CO2/g TOC)
I
II
III

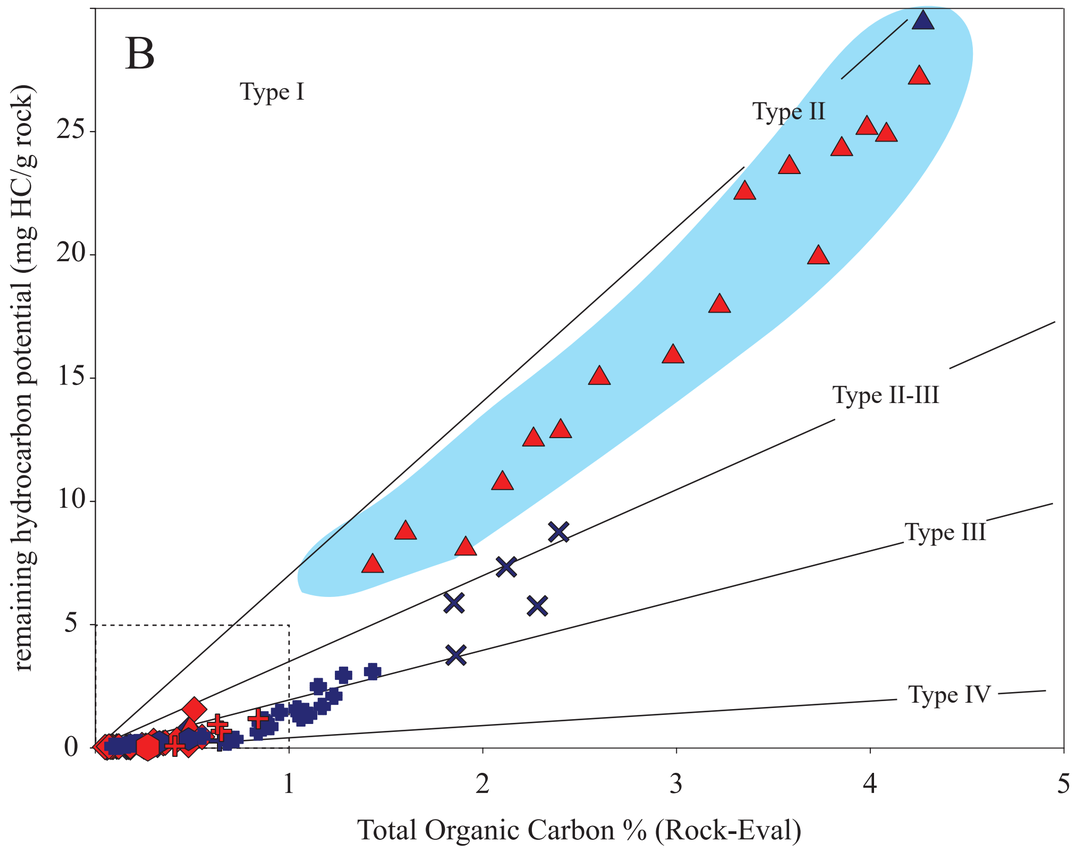
B
remaining hydrocarbon potential (mg HC/g rock)
Total Organic Carbon % (Rock-Eval)
Type I
Type II
Type II-III
Type III
Type IV

Fig. S5

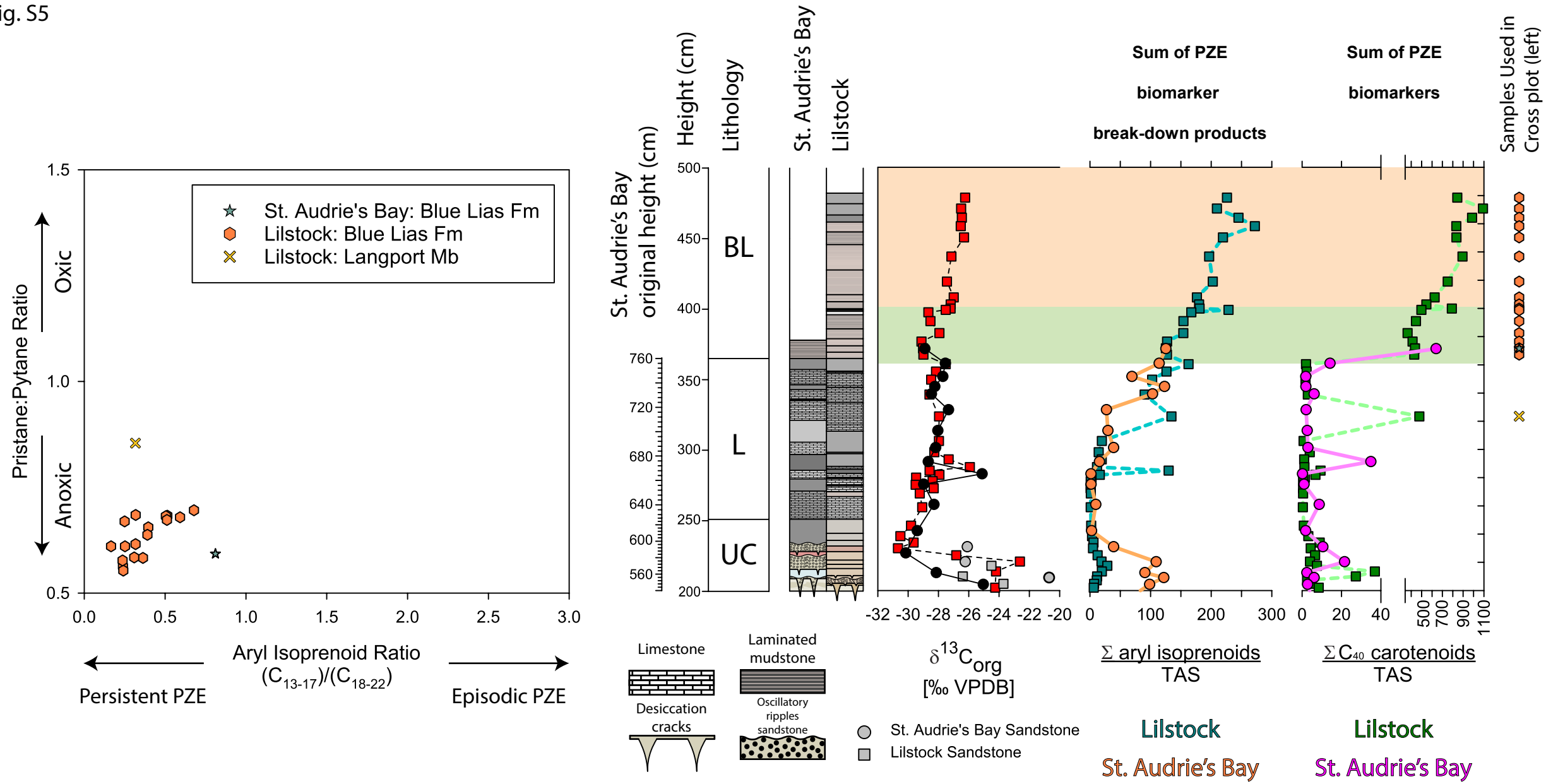
St. Audrie's Bay: Blue Lias Fm
Lilstock: Blue Lias Fm
Lilstock: Langport Mb
Pristane:Pytane Ratio
Oxic
Anoxic
1.5
1.0
0.5
0.0
0.5
1.0
1.5
2.0
2.5
3.0
Aryl Isoprenoid Ratio
(C13-17)/(C18-22)
Persistent PZE
Episodic PZE
St. Audrie's Bay original height (cm)
Height (cm)
Lithology
St. Audrie's Bay
Lilstock
BL
L
UC
760
720
680
640
600
560
500
450
400
350
300
250
200
Sum of PZE biomarker break-down products
Sum of PZE biomarkers
Samples Used in Cross plot (left)
-32 -30 -28 -26 -24 -22 -20
δ13Corg [‰ VPDB]
0 100 200 300
Σ aryl isoprenoids TAS
0 20 40
500 700 900 1100
ΣC40 carotenoids TAS
Limestone
Laminated mudstone
Desiccation cracks
Oscillatory ripples sandstone
St. Audrie's Bay Sandstone
Lilstock Sandstone
Lilstock
St. Audrie's Bay
Lilstock
St. Audrie's Bay

Fig. S6

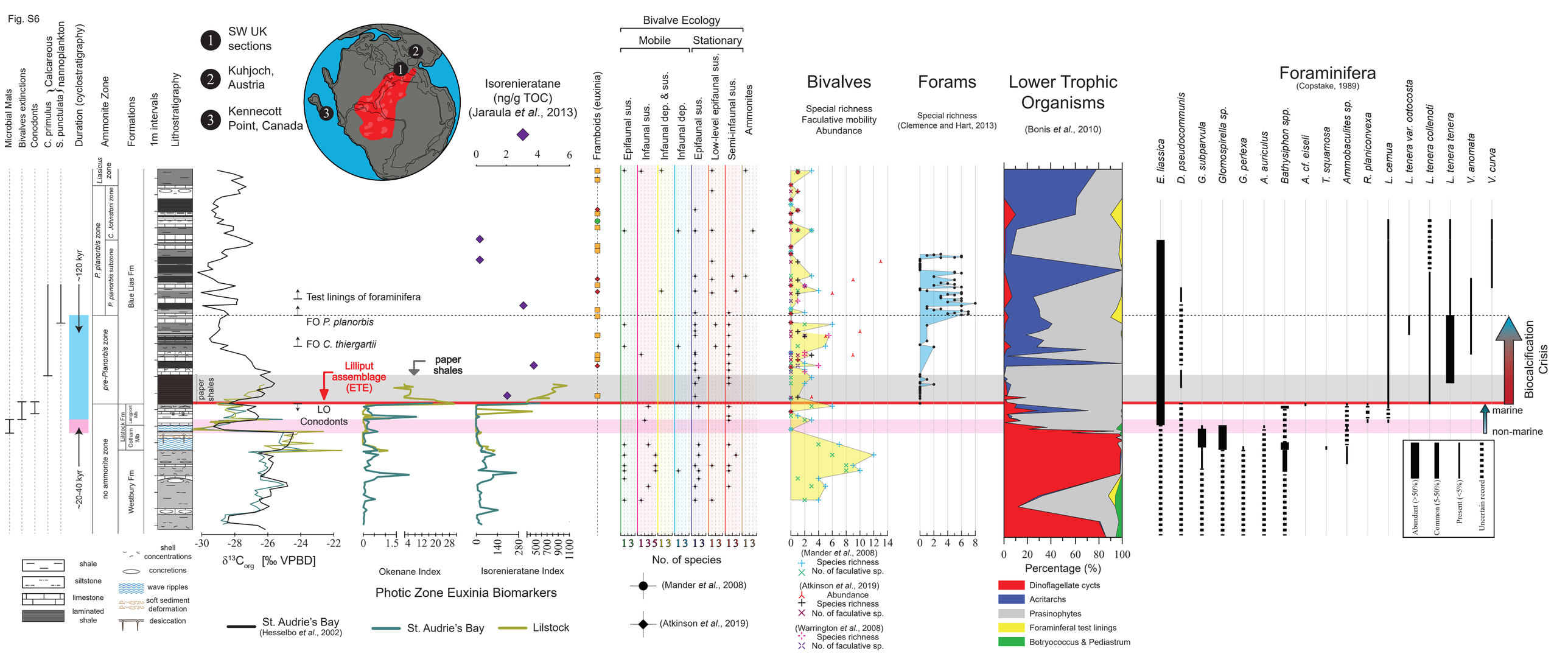
Microbial Mats
Bivalves extinctions
Conodonts
C. primulus
S. punctulata
Calcareous nannoplankton
Duration (cyclostratigraphy)
Ammonite Zone
Formations
1m intervals
Lithostratigraphy
1 SW UK sections
2 Kuhjoch, Austria
3 Kennecott Point, Canada
Isorenieratane (ng/g TOC) (Jaraula et al., 2013)
Framboids (euxinia)
Bivalve Ecology
Mobile
Stationary
Epifaunal sus.
Infaunal sus.
Infaunal dep. & sus.
Infaunal dep.
Epifaunal sus.
Low-level epifaunal sus.
Semi-infaunal sus.
Ammonites
Bivalves
Special richness
Facultative mobility
Abundance
Forams
Special richness
(Clemence and Hart, 2013)
Lower Trophic Organisms
(Bonis et al., 2010)
Foraminifera
(Copstake, 1989)
E. liassica
D. pseudocommunis
G. subparvula
Glomospirella sp.
G. perlexa
A. auriculus
Bathysiphon spp.
A. cf. eiseli
T. squamosa
Ammobaculites sp.
R. planiconvexa
L. cemua
L. tenera var. ootocosta
L. tenera collenoti
L. tenera tenera
V. anomata
V. curva
~120 kyr
~20-40 kyr
Liasicus zone
P. planorbis zone
C. Johnstoni zone
P. planorbis subzone
pre-Planorbis zone
no ammonite zone
Blue Lias Fm
Lilstock Fm
Cotham Mb
Langport Mb
Westbury Fm
paper shales
Test linings of foraminifera
FO P. planorbis
FO C. thiergartii
Lilliput assemblage (ETE)
LO Conodonts
paper shales
Biocalcification Crisis
marine
non-marine
Abundant (>50%)
Common (5-50%)
Present (<5%)
Uncertain record
shale
siltstone
limestone
laminated shale
shell concentrations
concretions
wave ripples
soft sediment deformation
desiccation
δ13Corg [‰ VPBD]
St. Audrie's Bay (Hesselbo et al., 2002)
Okenane Index
Isorenieratane Index
Photic Zone Euxinia Biomarkers
St. Audrie's Bay
Lilstock
No. of species
(Mander et al., 2008)
(Atkinson et al., 2019)
(Mander et al., 2008)
Species richness
No. of faculative sp.
(Atkinson et al., 2019)
Abundance
Species richness
No. of faculative sp.
(Warrington et al., 2008)
Species richness
No. of faculative sp.
Percentage (%)
Dinoflagellate cycts
Acritarchs
Prasinophytes
Foraminiferal test linings
Botryococcus & Pediastrum